Revista Brasileira de Física Médica.2011;5(3):233-38.

Simulated intensity profiles for cylindrical objects in magnification mammography: the effect of the spectrum

Simulação de perfis de intensidade de objetos cilíndricos em mamografia com amplificação: o efeito do espectro

Karla-Denaly Palma-Alejandro[1], Alberto Valdeolivas[2], Tatiana Alieva[3], Margarita Chevalier[2], Eduardo Guibelalde[2] and María-Ester Brandan[1]

[1]Instituto de Física, Universidad Nacional Autónoma de México – DF, Mexico.
[2]Facultad de Medicina, Universidad Complutense de Madrid – Madrid, Spain.
[3]Facultad de Ciencias Físicas, Universidad Complutense de Madrid – Madrid, Spain.

Abstract

We present a user-friendly Matlab® simulation interface tool to predict intensity profiles for magnified X-ray images of weakly attenuating cylindrical objects, including phase effects. Based on a previous monoenergetic formalism, we now consider polyenergetic X-ray beams and we study the effect of the spectral description on the predicted phase contrast. It was found that, for weakly attenuating objects with diameters $<\approx 1$ mm, detailed resolution in the spectrum description is not necessary. Simulations are compared with images of cylindrical objects, which were obtained under conditions found in a commercial digital mammography system. The magnification images of phantom plastic fibers show weak, however visible, edge enhancement due to phase contrast. The polyenergetic simulations provide an improved description of the data with respect to the effective energy monoenergetic assumption.

Keywords: phase contrast, edge enhancement, X-ray spectra, digital mammography, image analysis.

Resumo

Apresentou-se uma ferramenta de simulação com interface amigável desenvolvida em Matlab® para prever os perfis de intensidade de imagens de raios X magnificadas de objetos cilíndricos de pouca atenuação, incluindo efeitos de fase. Com base no formalismo monoenergético anteriormente desenvolvido, considera-se agora os feixes de raios X polienergéticos e estuda-se o efeito da descrição espectral no contraste de fase previsto. Para objetos de pouca atenuação, com diâmetros $<\approx 1$ mm, verificou-se que a resolução detalhada na descrição do espectro não é necessária. Imagens de objetos cilíndricos obtidas em sistemas de mamografia digital comerciais foram comparadas às simulações. As imagens de magnificação de fibras plásticas empregadas como simuladores mostraram pouco, porém visível, realce de borda devido ao efeito de contraste de fase. As simulações dos feixes polienergéticos forneceram uma melhor descrição dos dados em relação à aproximação de feixes monoenergéticos.

Palavras-chave: contraste de fase, realce de borda, espectros de raios X, mamografia digital, análise de imagem.

Introduction

X-ray phase contrast (PC) imaging is perceived as a powerful tool for imaging weakly attenuating objects[1-11], expected to represent a breakthrough in Diagnostic Radiology.

Conventional X-ray relies on differences in attenuation between tissues to produce the image. However, the interaction of X-rays with matter also leads to changes of the electromagnetic wave phase, which can be radiologically visible under certain conditions[3,6,8,10,11]. PC provides a better visualization of the edges, due to the gradient of the real part of the refraction index between materials. Phase changes induce interference and generate bright and dark stripes around object edges. This effect is complementary to the contrast produced by attenuation. Both properties are contained in the medium complex refractive index n, which, for X-rays, can be expressed as $n=1-\delta+i\beta$, where δ is the index of refraction decrement that describes the X-ray phase shift, and the imaginary part β is responsible for the attenuation. The macroscopic phase shift of the X-rays after propagating in a given material is directly proportional to the integral of δ over the trajectory. The β component of n takes into account the added probabilities of Rayleigh, photoelectric and Compton interactions, and

Corresponding author: María-Ester Brandan – Instituto de Física, Universidad Nacional Autónoma de México – Circuito de la Investigación Científica, s/n, Ciudad Universitaria – Coyoacán 04510 – México (DF), México – E-mail: brandan@fisica.unam.mx

it is directly proportional to the macroscopic linear attenuation coefficient μ[12].

Two requirements are necessary to observe the PC: the radiation field must have a certain degree of spatial coherence at the object position, and the detector must be placed at a certain distance away from the object (magnification conditions), for the interference fringes to be visible[1-11]. PC can be of relevance to radiological images of soft tissues, particularly in mammographic images, where certain breast tissues attenuate X-rays similarly. Some publications have reported the possible use of PC imaging for mammography clinical applications[6,9].

The radiological image of a cylinder is of particular interest, since blood vessels and other ducts in human anatomy have a cylindrical shape. Plastic fibers (with diameters <1 mm), which simulate vasculature of the mammary gland, are currently used in quality control phantoms for mammography systems, and edge enhancement in cylindrical objects has been observed using polychromatic X-ray spectra[7,10,11].

Previously[10,11], we have reported PC effects in the magnification images of plastic fibers inserted into the TORMAM mammography phantom[13], which was acquired with a Hologic Selenia mammographic unit (70 μm pitch size detector). These observations have been interpreted by a diffraction-based simulation, assuming a monoenergetic X-ray beam.

Olivo and Speller have presented a formalism[5] to simulate PC effects in magnification images of plastic fibers, taking into account the X-ray spectrum. They predicted a weak dependence, which is validated using an experimental arrangement optimized for the observation of PC effects. Based on our previous monoenergetic formalism[10,11], the aim of this work was to consider polyenergetic beams to study the effect of the spectral description on the predicted PC effects and to compare them with data obtained under magnification conditions available in a clinical mammography unit.

Materials and methods

Spectral resolution

Polyenergetic X-ray spectra, typical of those used in mammography, have been simulated following the formalism developed by Boone, Thomas and Jennings[14]. The spectrum is parameterized by a third-order polynomial dependent on the tube operating voltage and the beam attenuation by filter materials is analytically taken into consideration.

Polynomial coefficients for same anode/filter/voltage combinations have been previously determined in the Medical Physics Laboratory at the UNAM Physics Institute[15]. The filtered spectra were binned (every 0.5 keV) to optimize the numerical computation time. Figure 1a shows two representative calculated spectra and Figure 1b illustrates the effect of different bin sizes on a molybdenum (Mo) spectra.

Numerical simulation

The formalism to simulate the detected intensity profile, presented by Chevalier et al.[11], is a two-dimensional theoretical treatment based on Fresnel diffraction theory restricted to weakly attenuating cylindrical objects, considering an incoherent, monochromatic, and extended X-ray source. Applying Van Cittert-Zernike theorem, we have obtained the mutual intensity at the object plane from the intensity distribution of the incoherent source[11]. An analytical solution for the normalized intensity at the detector plane of a radiation field after passing through the object is derived in paraxial approximation. The detector response effect is introduced by the measured modulation transfer function (MTF).

In the polyenergetic simulation, we have calculated the profile for each energy bin using the relative photon fluence from zero to the maximum energy. Energy-dependent real and imaginary index of refraction values for polypropylene are obtained and interpolated from Henke, Gullikson and Davis[16], and those for nylon are calculated using the online resources in the same paper mentioned[16], assuming $C_6H_{11}NO$ composition and density 1.14 g cm^{-3} (average for nylon[17]). For nylon, δ and β values are 1.045E-05 and 5.106E-08 at 5 keV, and 2.882E-07 and 9.375E-11 at 30 keV, respectively. Typically within this energy range, δ (β)

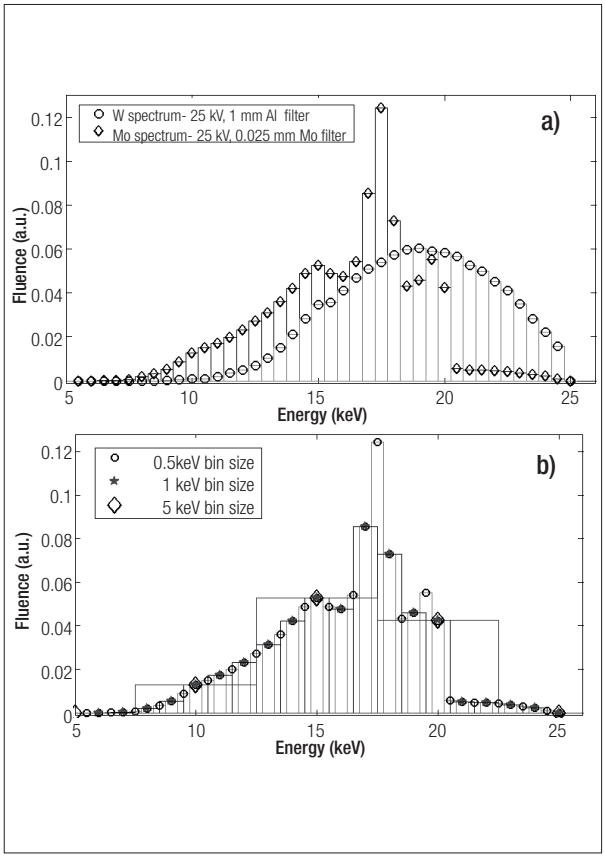

Figure 1. (a) Calculated energy spectra for W and Mo anodes, 25 kV, using Al or Mo filters (0.5 keV bin size); (b) molybdenum spectra, 25 kV, 0.025 mm Mo filter, for different bin sizes.

for nylon is 1.2 (1.6) times that for polypropylene. The object diffraction pattern is the incoherent sum of discrete profile intensities, normalized to the background[18]. Fast Fourier Transform (FFT) of the pattern is numerically obtained and multiplied by the detector MTF to include the effect of spatial resolution in the image receptor. Inverse FFT of the product is the simulated object intensity profile (Figure 2).

To facilitate the use of this simulation, a Matlab tool has been developed as a user-friendly interface (called Sook'Oochel-Prof Sim, Figure 3) offering the choice between anodes (W and Mo) and filters (Al, Mo, and Nb). It also offers the choice between a type of material (polypropylene and nylon) for the fiber composition. This tool displays the spectrum according to the selected number of bins as well as the simulated intensity profile, allowing graphical and numerical storage of the results.

Comparison with data

Simulations are compared with profile intensity measurements obtained in a Hologic Selenia digital mammography system, 100 μm nominal focal spot, 26 kV nominal operating voltage, Mo anode, Mo filter (0.025 mm thick), 25 cm source-object distance and 65 cm source-detector distance (i.e., magnification=2.6), and 10 mm long cylindrical fibers of diameter between 0.20 and 0.40 mm[11]. Fibers were those in the TORMAM phantom[13]. For each thickness, four fibers are arranged in a "chicken foot" geometry, one "horizontal" fiber, one "vertical", and two at ±45º with respect to the vertical central fiber. The phantom was manually positioned so that central fibers were parallel (within 0.5–1.5º) to the cathode-anode axis, and the fiber groups were located close to the radiation field central axis.

The edge enhancement (percentage) was quantified by the following expression (Eq. 1):

$$EE = 100\frac{I_{max} - I_0}{I_0} \quad (1)$$

Results and discussion

Spectral resolution

Figure 4 shows intensity profiles simulated for the experimental conditions described for different choices of bin size. In general, the U-shaped attenuation profile expected for a cylindrical object has been modified at the edges, due to phase effects[5,11].

The object attenuation at the center of the fiber is about 3%, and the edge enhancement is about 1% outside the object border. The predictions converge for bins smaller than 3.7 keV (in a 26 keV spectral interval).

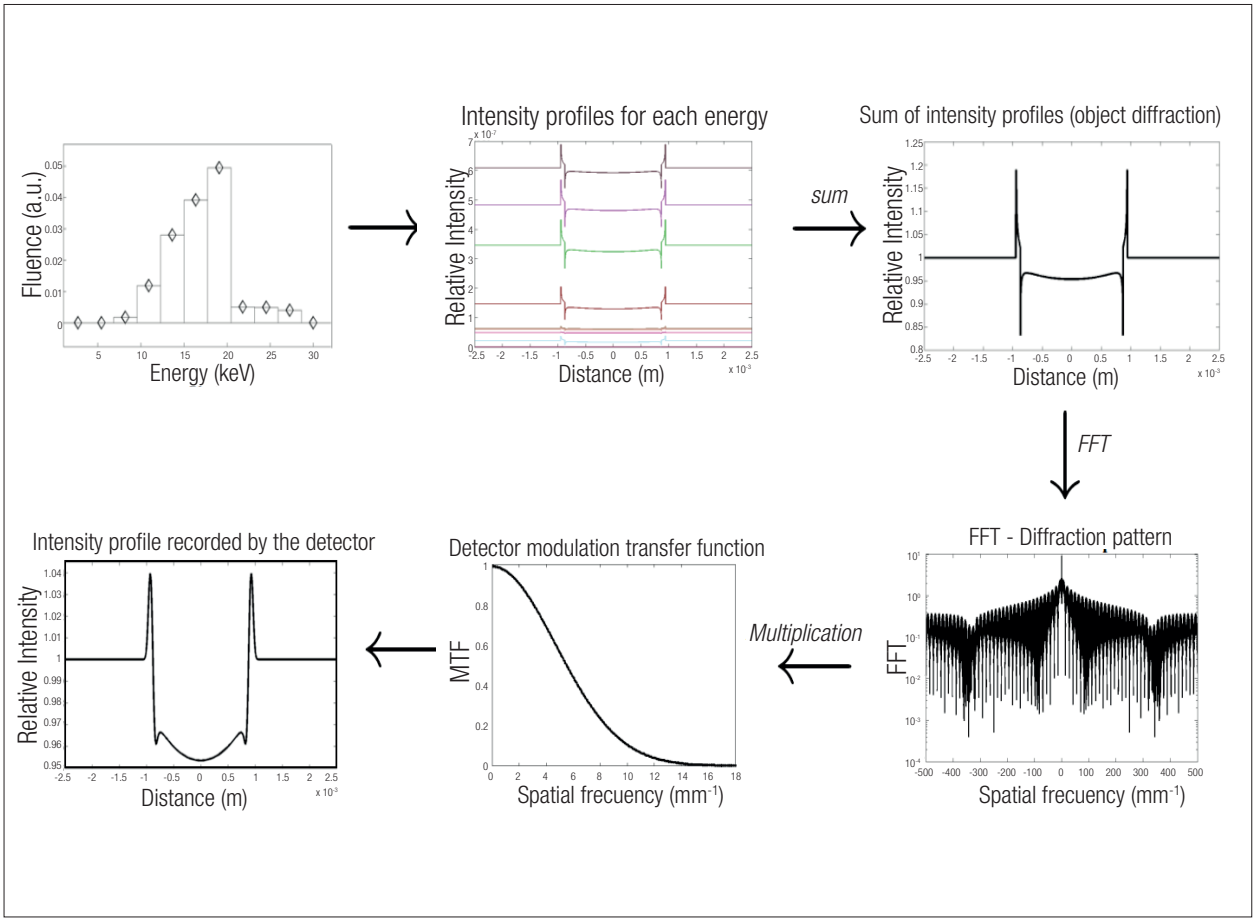

Figure 2. Simulation algorithm. The example corresponds to a 0.8 mm diameter fiber, magnification=2.0 and Mo/Mo 30 kV X-ray spectrum.

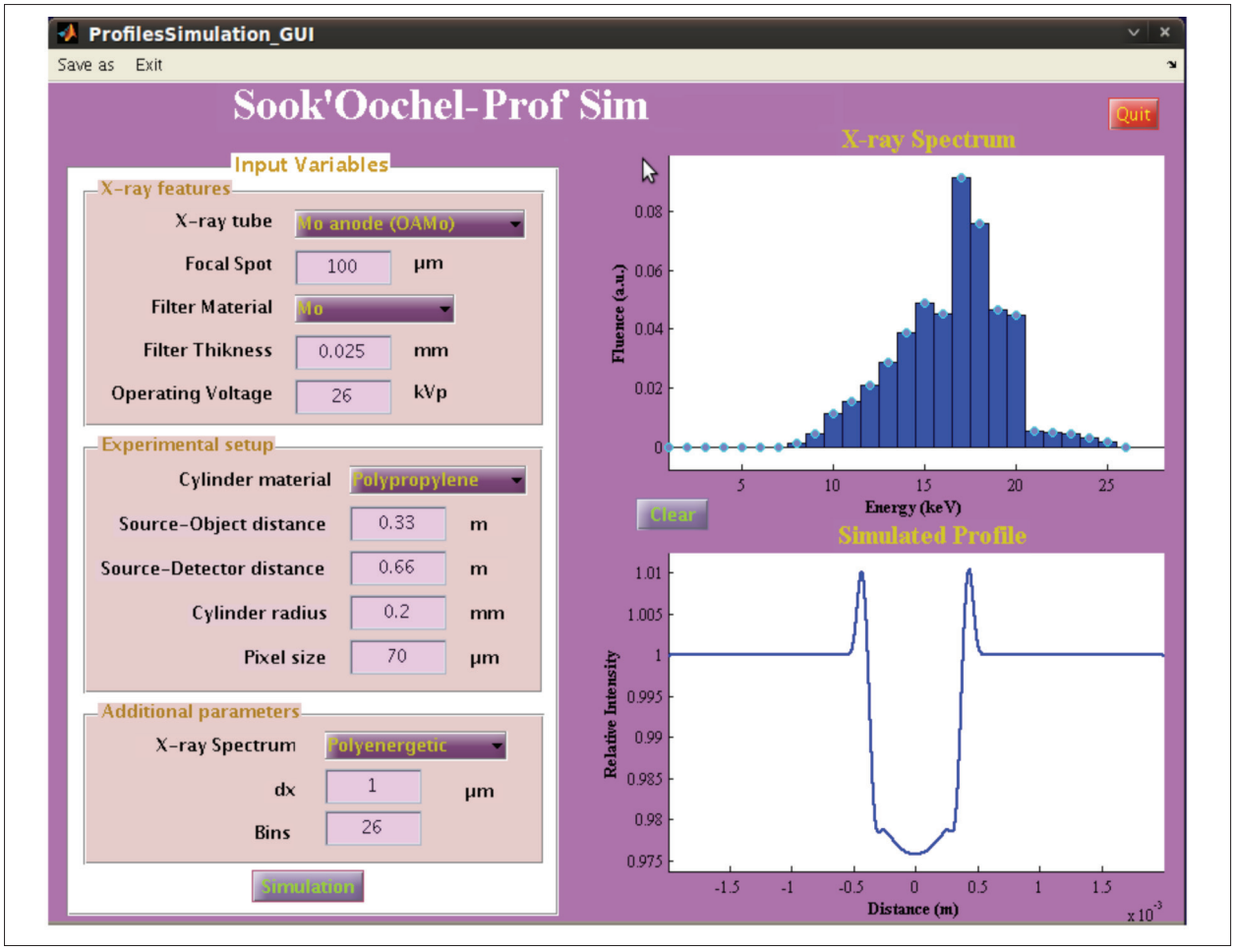

Figure 3. User interface (called Sook'Oochel-Prof Sim) for intensity profile simulation.

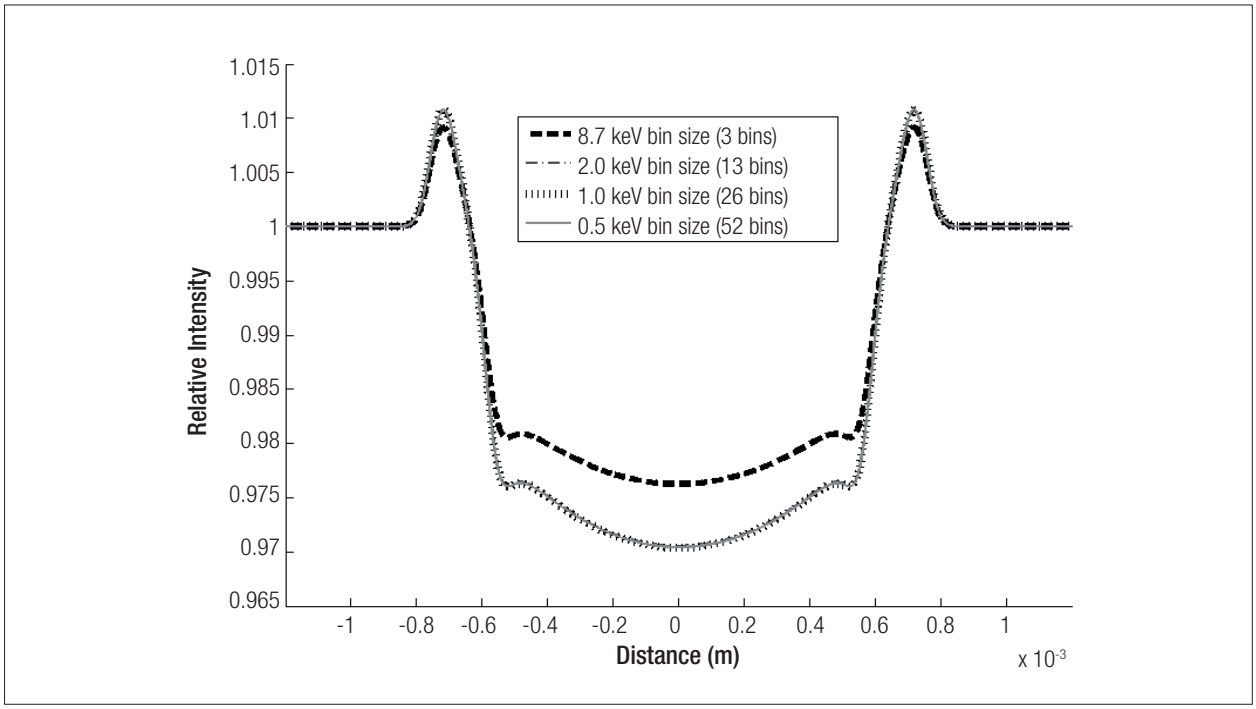

Figure 4. Intensity profiles for a 0.6 mm diameter polypropylene fiber, Mo anode, 0.025 mm Mo filter, magnification=2.0, polyenergetic spectra, 26 kV, different energy bin sizes.

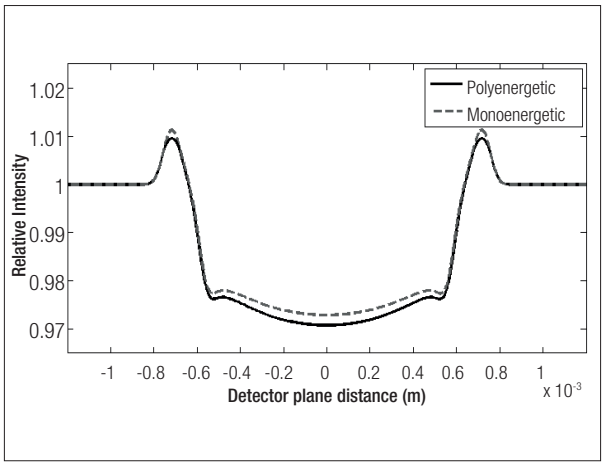

Figure 5. Simulated intensity profiles for a 0.6 mm diameter polypropylene fiber, magnification=2.0. Solid curve is for a Mo/Mo spectrum (26 kV-3.7 keV bins) and dashed curve is for a 15 keV monoenergetic spectrum.

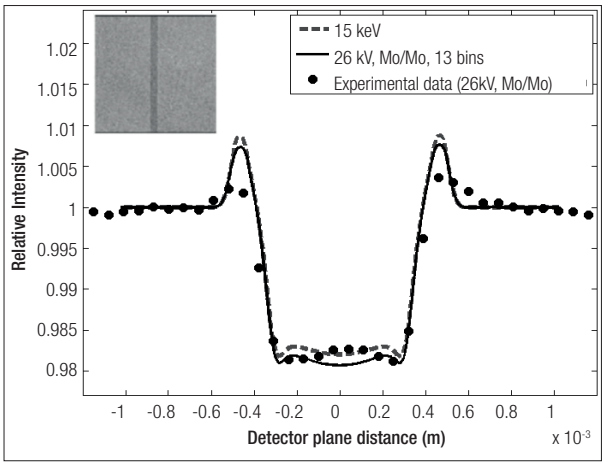

Figure 6. Data[11] and simulation for the 0.3 mm diameter fibers, including the one shown in the inset. Symbols are the data, dashed curve is monoenergetic (at effective energy 15 keV), and solid curve is the polyenergetic intensity simulation of a nylon fiber at magnification equal to 2.6.

Simulations as a function of the spectrum

Figure 5 compares the mono- and polyenergetic simulations. For the monoenergetic case, the effective energy of the X-ray beam (evaluated from half-value layer measurements[11]) was used. Predicted edge enhancement is about 1.1% above the background for the monoenergetic case; this value decreases to about 0.9% if the complete spectrum is considered. Differences of similar magnitude are visible at the fiber center, where use of the complete spectrum reduces the transmission by about 0.2%.

Even if the values of δ and β vary strongly over the energies relevant to these simulations, the observed features in the simulated fiber profile show a relatively weak dependence on the consideration of the polyenergetic spectrum. These predictions of a weak effect agree qualitatively with the previously mentioned results[5], which were obtained with similar X-ray spectra under experimental conditions optimized for the observation of phase effects.

Comparison with data

Figure 6 shows the measured intensity profile of the 0.3 mm diameter group of fibers at magnification=2.6. This profile is the average of the measurements for the central and ±45º fibers of the group (profiles for the three fibers were quantitatively similar and they were averaged to reduce intensity fluctuations). For comparison, the mono- and polyenergetic simulations are also shown. Simulations reproduce the loss of the U-shaped attenuation and the presence of edge enhancement, both due to phase effects. Data display an edge enhancement of about 0.4% above background and calculations predict a ≈0.8% effect (0.75% polyenergetic and 0.85% by the monoenergetic simulation). The quantitative disagreement between data and simulations displayed in Figure 6 (observations are about 50% of predictions) occurs for all fiber diameters. A possible explanation could be the presence of scattered radiation, unaccounted for in the formalism. The polyenergetic simulation improves the agreement with the observations, but it still overpredicts the magnitude of the effect external to the edge.

Conclusions

We have presented a versatile Matlab simulation tool to predict intensity profiles for magnified images of cylindrical objects obtained under conditions, which permit PC effects to be visible.

We have found that, for objects with diameters <1 mm, the detailed resolution in the spectrum description is not necessary. We have obtained an improved description of the data in the polyenergetic simulation, with respect to the assumption of a single effective energy. However, this improvement is still insufficient to reach a quantitative agreement with observations. On the other hand, the measured profile shape is well-described by the simulation.

Observations and calculations of PC effects are small (≈1% edge enhancement), nevertheless of interest for conditions found in a commercial mammographic unit.

Acknowledgments

Authors acknowledge partial support from Universidad Nacional Autónoma de México (UNAM), grant PAPIIT-IN102610. TA acknowledges the financial support of the Spanish Ministry of Science and Innovation, under project TEC2008-04105. KDPA acknowledges support from Consejo Nacional de Ciencia y Tecnología, CONACyT-Mexico, for postgraduate studies scholarship.

References

1. Fitzgerald R. Phase-sensitive X-ray imaging. Physics Today. 2000;53(7):23-6.
2. Lewis RA, Rogers KD, Hall CJ, Hufton AP, Evans S, Menk RHE, Tromba G, et al. Diffraction-enhanced imaging: improved contrast and lower dose X-ray imaging. Proceedings of the SPIE (Medical Imaging). San Diego, CA, USA: SPIE; 2002. p. 286-97.
3. Lewis RA. Medical phase contrast X-ray imaging: current status and future prospects. Phys Med Biol. 2004;49(16):3573.
4. Wilkins SW, Gureyev TE, Gao D, Pogany A, Stevenson AW. Phase-contrast imaging using polychromatic hard X-rays. Nature. 1996;384: 335-8.
5. Olivo A, Speller R. Polychromatic phase contrast imaging as a basic step towards a widespread application of the technique. Nulc Instr Meth A. 2007;580:1079-82.
6. Kotre CJ, Birch IP. Phase contrast enhancement of X-ray mammography: a design study. Phys Med Biol. 1999;44(11):2853.
7. Yadava PS, Yogesh K, Sarkar PS, Amarinha S, Godwal BK. Study of phase contrast imaging for carbon fiber, polystyrene and lung tissue using monochromatic and polychromatic X-ray sources. Nucl Instr and Meth A. 2006;564:496-505.
8. Ingal VN, Beliaevskaya EA, Brianskaya AP, Merkurieva RD. Phase mammography - a new technique for breast investigation. Phys Med Biol. 1998;43(9):2555.
9. Yamazaki A, Ichikawa K, Kodera Y. Investigation of physical image characteristics and phenomenon of edge enhancement by phase contrast using equipment typical for mammography. Med Phys. 2008;35(11):5134-50.
10. Brandan ME, Chevalier M, Guibelalde E, Rodrigo JA, Alieva T. Observation of edge-enhancement in digital images obtained with a clinical mammography unit. In: Olaf Dössel, Wolfgang C. Schlegel, editors. Proceedings of the World Congress on Medical Physics and Biomedicine. Munich, Germany. Berlin: Springer Heidelberg; 2009. p. 331-4.
11. Chevalier M, Chanes L, Guibelalde E, Brandan ME, Alieva T. Influence of geometrical factors on phase contrast fiber images. In: Martí J, Oliver A, Freixenet J, Martí R, editors. Proceedings of the Digital Mammography-IWDM. Girona, Spain. Berlin: Springer-Verlag Heidelberg; 2010. p. 334-41.
12. Gundogdu O, Nirgianaki E, Che Ismail E, Jenneson PM, Bradley DA, Benchtop phase contrast X-ray imaging. Appl Radiat Isot. 2007;65:1337-44.
13. Cowen AR, Brettle DS, Coleman NJ, Parkin GJS. A preliminary investigation of the imaging performance of photostimulable phosphor computed radiography using a new design of mammographic quality control test object. Br J Radiol. 1992;65:528-35.
14. Boone JM, Thomas RF, Jennings RJ. Molybdenum, rhodium, and tungsten anode spectral models using interpolating polynomials with application to mammography. Med Phys. 1997;24(12):1863-74.
15. Moya UE, Brandan ME, Martínez-Dávalos A, Ruiz-Trejo C, Rodríguez-Villafuerte M. Parameterization of X-ray spectra appropriate for microCT scanners. Nucl Instr Meth. 2010;613(1):152-5.
16. Henke BL, Gullikson EM, Davis JC. X-ray interactions: photoabsorption, 545 scattering, transmission, and reflection at E = 50-30000 eV, Z = 1-9. Atomic data and nuclear data tables 1993. [cited 2010 october]. Available from: http://henke.lbl.gov/optical_constants/getdb2.html.
17. MatWeb Material Property Data, Overview of materials for Nylon 66, Unreinforced. 1999. [cited 2011 November]. Available from: http://www.matweb.com/search/DataSheet.aspx?bassnum=O2500&group=General
18. Born M, Wolf E. Principles of Optics. Oxford: Pergamon; 1980.